AUT Journal of Mechanical Engineering

AUT J. Mech. Eng., 1(1) (2017) 55-66
DOI: 10.22060/mej.2017.12249.5289

A Geometric Modeling Approach to Find the Best Microstructure for Infiltrated SOFC Electrodes

M. Tafazoli[1], M. Shakeri[1*], M. Baniassadi[2], A. Babaei[3]

[1] Mechanical Engineering Department, Babol Noshirvani University of Technology, Babol, Iran
[2] School of Mechanical Engineering, College of Engineering, University of Tehran, Tehran, Iran
[3] School of Metallurgy and Materials Engineering, College of Engineering, University of Tehran, Tehran, Iran

ABSTRACT: In this study, a novel design paradigm is presented to obtain some geometry-related electrochemical and physical properties of an infiltrated SOFC electrode. A range of digitally realized microstructures with different backbone geometric properties and virtual electro-catalyst particle loadings under various deposition conditions are generated. Triple Phase Boundary (TPB), the active surface density of particles and gas transport factor are evaluated in those realized models based on selected infiltration strategy. Based on this database, a neural network is trained to relate the desired range of input geometric parameters to a property hull. The effect of porosity and geometric anisotropy in backbones in addition to the loading, distribution and aggregation behavior of particles is systematically investigated on those performance indicators. The results indicated that microstructures with very high amount of TPB and contact surface density of particle have a relatively low gas diffusion factor, meanwhile increasing these parameters does not involve a sensible contradiction. Also, by adding particles, the TPB density variation is changed as a function of backbone porosity and the average shape of aggregated particles. A direct search into the microstructure and property hull is applied to find the best parameters in modeling approach aiming the maximum effective geometric properties. Finally, a genetic algorithm is employed to detect appropriate geometric factors getting the maximum acquirable performance in infiltrated SOFC electrodes.

Review History:
Received: 14 December 2016
Revised: 1 March 2017
Accepted: 16 April 2017
Available Online: 17 April 2017

Keywords:
Microstructure optimization
Infiltrated electrode
Realization of microstructure
Solid oxide fuel cell

1- Introduction

Growing demands for energy has attracted international research efforts and led them to the cleaner energy sources. Research on the fuel cell, as a sustainable energy source, has shown high interest and generated considerable expectations over the last decades [1, 2]. These devices allow for the efficient transformation of fuel into electrical power and eliminate CO2 emissions by converting H2 as fuel to water as by-product. Solid Oxide Fuel Cells (SOFCs) are among the most efficient devices for direct conversion of fuels into electrical energy with the minimal environmental impact [3]. Performance and durability of an SOFC electrode are directly related to the geometric characteristics of its microstructure [4,5]. Improving microstructural properties such as Triple Phase Boundaries (TPBs) and effective transport pathways directly promote the electrochemical reactions and reactant movement. Thus, it should be understood to develop optimum electrodes with a higher performance [6]. The recent development of more sophisticated microstructural characterization tools has now enabled researchers to explore microstructure of SOFC by investigating the complex interplay between gas and solid phases and their relationship to performance [5]. Direct imaging of three-dimensional SOFC electrode microstructure with focused ion beam scanning electron microscopy (FIB-SEM) and X-ray computed tomography (XCT) now could be used to obtain quantitative measures such as TPB length and tortuosity factor [7]. In addition to the experimentation, a numerical simulation can be employed to obtain a detailed 3D insight into how SOFC electrodes function. The modeling efforts have led us to a better understanding of local phenomena taking place at the microstructure scales, for instance, local potential distribution inside the electrode and its effect on reaction kinetics and physical properties such as ionic or electronic conductivities, and, therefore, to further improve electrode performance and reliability [5,8]. These morphological parameters sometimes have inconsistent and nonlinear behaviors such that a small increase in one may result in a detrimental effect on others. For example, the tortuosity of pathways within each phase directly affects the transport to and from TPBs [9]. To overcome these complications, Joen et al. [10] first introduced a micro scale model for the microstructure and performed a numerical optimization on the microstructure of the anode supported SOFC. In particular, they investigated the dependence of the electrochemical reaction and the mass transport on the particle size and thickness of the functional layers of the electrode and reported that a smaller particle size for cathode functional layers enhances the electrochemical performance and deteriorates mass transport efficiency simultaneously. Based on these findings, the thickness of the cathode functional layers should be reduced in accordance with the particle size to maintain the mass transport resistance in the same level.

Nanostructured materials such as infiltrated electrodes are the key to enhance fuel cell performance. These fuel cells are usually made of a backbone microstructure with particles deposited on them by infiltrating/impregnating methods. Designing optimal microstructures and achieving them by controlling the material and manufacturing process, and

Corresponding author, E-mail: shakeri@nit.ac.ir

maintaining the optimum microstructure during the fuel cell operation are problems that attract many research works. Because of the effects of microstructure geometry on the physical or electrochemical properties of electrodes and their interactions, a geometric model can be useful to predict these phenomena. More recently, a nanostructured electrode made by infiltration techniques has been the center of attention in the SOFC research community. Easier control of composition and particle sizes are the major reasons for the better performance of infiltrated electrode than conventional electrodes. In this process, the porous structure (scaffold) is first fabricated on top of the dense electrolyte and then another solid phase is introduced in the form of particles that leads to a significant boost in the TPB density for the electrode microstructure. A summary of the history and the latest developments in infiltration techniques for this application can be found in [11, 12].

Thanks to the recent progress in micro/nano-imaging and characterization methods accompanied by introducing more advanced computational techniques that have made it possible to simulate the nanostructured electrodes. For instance, Zhang et al. [4] developed a model to construct a 3D microstructure of infiltrated SOFC electrodes. In their study, the generation of backbone microstructure has been carried by randomly dropping spherical particles on the surface of backbone. Based on this geometric model, they have reported the geometric properties of the electrode, including the percolation threshold of infiltrated nanoparticles and pores, TPB length, nanoparticles surface area, backbone surface area and interfacial area between the backbone and nanoparticles. They have also systematically reported the effects of particle size, backbone porosity, infiltrated particle size and its aggregation risk. In another work, Zhang et al. [13] have developed a model for the dual-phase infiltration procedure. Bertei et al. [14] have developed a numerically reconstructed model for infiltrated electrodes by employing a sedimentation algorithm for the backbone generation and a novel Monte-Carlo packing algorithm for the random infiltration. Their study shows that the electrodes made by infiltration may show up to two orders of magnitude increase in TPB density compared to conventional composite electrodes. Synodis et al. [15] have presented a mechanistic model to predict both the percolation threshold and effective conductivity of the infiltrated SOFC electrodes. In this study, model predictions are compared to two separate published experimental studies and it is shown that effective conductivities and percolation thresholds can be varied by infiltrating particle size, pore size, and porosity. To predict the dependence of effective electronic conductivity and active TPB length on experimentally controllable and measurable parameters, Hardjo et al. [16] have developed an effective property model for infiltrated electrodes. They presented a methodology to relate an experimentally observed degradation in the effective electronic conductivity of infiltrated electrodes to a reduction in active TPB length as a function of time. A mechanistic model to predict the active TPB density, in combination with an effective conductivity of infiltrated SOFC electrodes is presented by Reszka et al. [17]. That study shows that the scaffold/infiltrate size ratio has the greatest impact on the TPB density, followed by the porosity and pore/infiltrate size ratio. Their model provides an insight over the rational design of infiltrated electrodes and conforms well to the experiment. Recently Kishimoto et al. [6] have studied the 3D microstructure of nickel-infiltrated gadolinium-doped ceria Ni /GDC electrodes using focused ion beam tomography by quantifying microstructural parameters of the actual electrode microstructure such as volume fraction, TPB density and mean particle/pore sizes. A comparison between the infiltrated electrodes and conventional electrodes indicates that the infiltrated electrodes have a greater potential to independently control metal particle size, porosity and TPB density, which is a significant advantage in developing optimal electrode microstructures. In addition, they have developed a one-dimensional numerical model to investigate the effect of the microstructural parameters on the effective transport coefficients and electrochemical reaction rate of the electrode [6, 18].

Investigation of complex input/output relationships in this kind of electrochemical devices needs an effective modeling method such as Artificial Neural Networks (ANNs). These networks like the human brain consist of a number of neurons with different transfer functions to correlate the multi input/output parameters in engineering problems [19-21]. Marra et al. [22] have used a neural network to estimate the SOFC performance. Also, Bozorgmehri et al. [23] have employed ANN and a Genetic Algorithm (GA) to model the effect of constructive parameters (anode porosity, electrolyte thickness, electrode support/functional layer thickness) of a single SOFC power density. Among the different types of ANNs, some researchers such as Saengrung et al. [24] investigated the performance of a commercial Proton Exchange Membrane (PEM) fuel cell system with the Back-Propagation Neural Network (BPNN) as a useful tool to quite satisfactory control of the output parameters based on the variations of input data. The performance of this method is determined by varying error goals, the number of neurons, the number of layers and training algorithms.

All of those geometric modeling studies have restricted their investigation in specific regions especially in determining the geometric properties of backbone and aggregation behavior of particles. To solve this problem, we presented a comprehensive framework in the current study to couple a new geometric modeling approach with the artificial intelligence approach. At first, a set of 3D microstructures with different porosities and geometric anisotropies are realized as backbones following a controlled Monte-Carlo method. Then, particles in the form of single voxels are added to the microstructures using a novel algorithm to simulate the various aggregation behaviors of infiltrating particles on the backbones. This process consisted of preliminary seeding and controlled deposition of particles. Unlike the above-mentioned modeling methods, in this study, the average geometry of particles on the surface of the scaffold can be controlled in addition to the particle loading. Controlling the distribution and agglomeration of particles on the scaffold have created new opportunities in our geometric design. In this paper, not only the TPB density and active surface area of particles were evaluated as the same as the other; but also the gas transport factor is evaluated by converting the realized microstructures to geometric models. In addition to those innovative methods in modeling and characterization procedure, since the realization of different electrode microstructures are so time-consuming and their characterization is a complex process; there is a need to develop a tool to estimate the effective properties of assumed

microstructures. It can be a practical solution to determine the limitation of microstructure properties and their interactions to create a general function to correlate the constructive parameters to those properties and perform an optimization process. Therefore, all of the input and output geometric data in this research are used to train a neural network and generate a set of possible microstructures with different effective properties named property hull. This includes a comprehensive set of effective property values predicted by sweeping input parameters within their range. The neural network was coupled with some multi-objective optimization methods to have a powerful search engine to find the best electrode microstructure in different scenarios. Additionally, this method prepares a comprehensive assessment of interactions among different properties such as reaction site density, reactant gas diffusion and conductivity of structural phases. In this study, a simple direct search method and a multi-objective genetic algorithm process are conducted to find the best microstructure on the base of different scenarios, which controls the most effective geometric-related electrochemical properties in the electrodes.

2- Microstructure Generation and Characterization

To achieve realistic microstructures, in this study we attempt to computationally replicate the real process of infiltrated electrode fabrication. In the first stage, a porous backbone microstructure will be generated based on the Monte-Carlo approach that is composed of three steps: i) generation, ii) distribution and iii) growth of the cells. In the first step, several initial seed cells are randomly placed in a unit cell of the electrode. Upon initial seed placement, the growth step starts following a cellular automation algorithm. This procedure continues till the desired volume fraction of each phase is achieved. From a different perspective, the growth step continues till all phases meet and fully occupy the grid. Penetration between the phases is avoided at all times throughout the initial distribution and growth of the cells [25]. This process can be controlled in different directions by adjusting axial or transversal grain growth rate with respect to the electrolyte. In Fig. 1 grain growth rate in backbones are adjusted to generate directional microstructures.

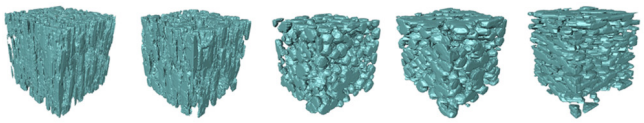

Fig. 1. 3D realized backbones with different geometric anisotropies (Axial grain growth rate -normal to the electrolyte-is reduced from left to right)

One of the most important aspects of this model is the size of the representative volume element (RVE) to obtain the microstructural behavior. To establish an applicable link between the RVE properties and full electrode model, statistical methods such as correlation function diagrams have been used in [26-28] to ensure the validity of results and the relationship between the size of RVE and voxelized space resolution. The line intercept method has been used to extract the average particle size of the solid phase in the backbone. Fortunately, it meets the criteria of a minimum number of particles (~7) should fit into the edge of RVE. In the following, to ensure the minimum number of voxels (~20) to divide those particles, the RVE size is selected to 150×150×150 voxels. As a result, the average particle diameter of backbone microstructure would be in the range of 500-750 nm that is in the normal range of powder grading in SOFC materials also it corresponded to the range of 20-30 nm for the length of voxel edge Length (L) that would be the minimum size of none agglomerated deposited particle.

After the generation and characterization of the backbone, as discussed in another study, particles will be added into the realized microstructures. Unlike the previously mentioned modeling approaches, which assumed the particles in the form of spheres or single cubic voxels, this proposed method can create a wide variety of geometric shapes on the surface of backbone electrode from aggregated particles. At first, a number of infiltrating particles, controlled by seeding ratio, were deposited on an active surface of backbone as preliminary seeds. This process can be accomplished completely randomly or as a function of some parameters such as backbone material or the surface geometry. In the next step, the rest of particles are deposited around the seeds. Depending on the modeling adjustments, agglomeration and dispersion of particles are controlled by the probability of particle deposition on the surface of pre-deposited seeds (low values of agglomeration rate) or on the backbone surface near the pre-deposited seeds (high values of agglomeration rate).

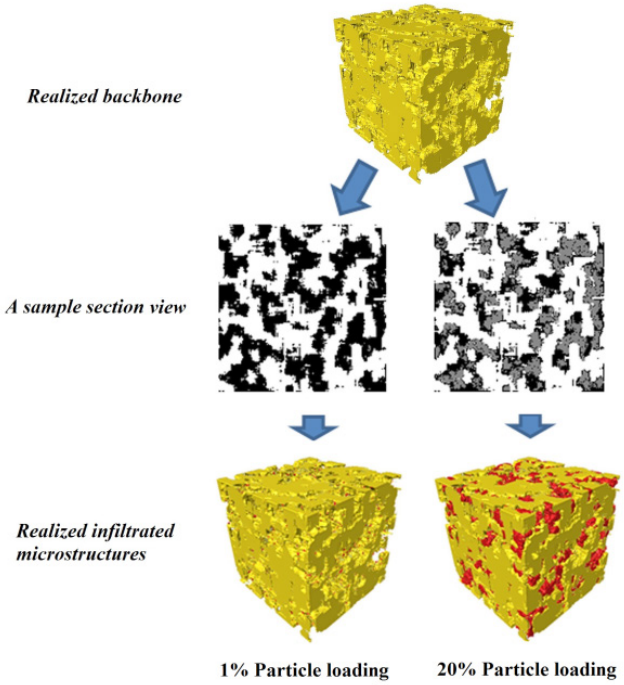

Fig. 2. 3D realized virtual infiltrated microstructures with 1% particle loading (left) and 20% volumetric loading (right)

The modeling parameters such as seeding and agglomeration ratio can be extracted from the position of voxels in digitized interior space of virtual skullcaps with different heights, contact diameters, and angles. These parameters might be extracted from digitized 2D cross section images with enough resolution to detect the average shape and amount of deposited particles phase on the surface of backbone. A sample of realized infiltrated microstructures with very low (1%) and high (20%) loading of particles is shown in Fig. 2.

When the realization of the models is completed, a wide range of geometric characteristics can be evaluated from the models. To narrow down the scope of this study, the most effective geometric parameters should be determined based on the material characteristics of electrode backbone and particles. Generally, there are three strategies in infiltration; in the first one, the backbone is made of electronically conductor material and the particles are made of ion conductor materials. The second strategy is vice versa, the scaffold is made of ion conductor material and the particles are electronically conductor. In these strategies, the most important reaction sites are TBBs and can be considered as a performance indicator, provide that the ionic conductivity is enough to transport the ions of the electrochemical reactions [29]. In the third strategy, the backbone is made of Mixed Ionic Electric Conductor (MIEC) material and a small part of electrochemical reactions can occur on Double Phase Boundaries (DPB) on the contact surface of scaffold and gas routes. In this kind of electrodes depending on the backbone material, the infiltrate particles can be made of electronically conductor material to elevated electrical conductivity or ionic conductor material to enhance the ionic conductivity of microstructure. In addition to this, they can be also made of the MIEC materials to raise the reaction sites on the contact surface of the electrode with reactant gases. However recently a large number of researchers have added highly electrochemically active materials (like Pd, Ru,...) to these electrodes to enhance the oxygen reduction on the surface of backbones via spillover mechanism. They could alleviate the polarization resistance by increasing the electrochemically active surface density of electrode. [11, 30-32]. Based on these findings, depending on the preferred strategy, the effective geometric properties for estimating the active density of electrochemical sites would be changed. In this study based on the third strategy, active surface density of particles and their triple phase boundary with the scaffold and the gas routes were selected as the electrochemical performance indicators. In addition to the abundance and effectiveness of reaction sites, the diffusivity of reactant gas is another important parameter especially in high current densities or high temperature working conditions. It can be a rate limiting phenomena in the electrode and a large number of TPBs and higher ionic conductivity cannot compensate the limitation of the gas diffusions in the performance of the cell [18]. Other important parameters such as ionic conductivity of backbone as well as the electric conductivity of deposited particles could be evaluated in this model, but it is assumed that they are not in a range which can affect the electrochemical performance significantly especially in the last infiltration strategy. As a result, the target function should be extracted from the role of materials in the microstructure based on the infiltration strategy. The in-process parameters such as temperature and current density are non-geometric parameters to determine the importance of each variable in that function.

- **TPB density**

As many studies report, like Janardhanan [1] , the density of active TPBs, where the ionic and electric conductor meets each other in reactant gas routes, plays a major role in the overall microstructure of the SOFCs and significantly affects the efficiency of the SOFC. As this interfaces between the phases, they play an essential role in the electrochemical performance of electrode [1]. In this study, we have updated the method of Cronin [2, 3] to calculate the TPB density using new acceptable neighborhood image patterns in virtually infiltrated microstructures.

- **Contact surface density of particles**

In addition to TPB calculation, some research works have suggested that double phase boundaries between deposited particles and active reactant gas routes can play an important role in electrochemical reactions especially highly active electrochemical particles on the surface of MIEC backbones [4, 5]. The implemented algorithm is started with the identification of all active contact surfaces on the backbone. Then the active surfaces of deposited particles as well as other contact surfaces between different phases are calculated by sorting special columns in identification matrix of realized microstructures.

- **Gas transport factor**

Another effective parameter in the performance of SOFC electrodes is the gas diffusion, especially in high current densities or high temperatures. Important factors characterizing the gas diffusion in porous media are the porosity and tortuosity of the gas routes [6]. Due to its simplicity, Fick's law is commonly adopted to assess gas diffusion. For porous media, Fick's first law can be modified by introducing porous media factors as

$$D_{ij}^{eff} = \frac{\phi}{\tau} D_{ij} \tag{1}$$

Where $D_{i,j}$ is binary diffusivity of the gas species, $D_{i,j}^{eff}$ is the effective binary diffusivity of the gas species, and ϕ and τ are the porosity and tortuosity, respectively. In this research, tortuosity is obtained from the effective thermal conductivity using Avizo XlabTM, EFI Corporation, For this purpose, the thermal conductivity of the pore network, K_{eff} is obtained by performing a thermal simulation and the tortuosity is calculated based on

$$\tau = \varepsilon \frac{K_{bulk}}{K_{eff}} \tag{2}$$

where we assume K_{bulk}=1.

As discussed by Zhao et al. [7], whenever the molecular distance of a gas is in the order of average pore size, the Knudsen diffusion should be directly considered. In the current study, this effect is neglected due to different orders of calculated average pore size (300–500 nm) in realized backbones. However the Knudsen diffusion can also affect the gas diffusivity but to simplify the optimization scheme, the gas transport factor is defined regardless of the average pore size and estimated in the porous electrodes by this equation:

$$GasTrasportFactor = \frac{\varepsilon}{\tau} \tag{3}$$

- **Microstructure Hull**

In traditional design, material and geometry are usually varied iteratively to meet the design requirements. A more efficient approach to design requires simultaneous material and geometry optimization. Following this approach for the design of material, a microstructure hull is needed which

consists of a set of possible microstructures existing within a region characterized by certain distribution functions obtained from the microstructure. In other words, a closure in this sense includes all possible effective property values predicted by sweeping input parameters defining these distribution functions, and generally, a solution is a subset of this closure. In the current study, it is assumed that if two points are chosen in the property space, they correspond to two points in the geometry space that are connected with a continuous path in both spaces. Although this may be judged as an over simplistic approach, it allows us to demonstrate the concepts. Let us select TPB density, contact surface density, and gas diffusivity as critical design objectives. Mathematically speaking, a property closure for these parameters can be obtained using an arbitrary analytical or approximate method and their boundaries represent constraints for the optimization process [39, 40].

3- Methodology

In this study, the realization of 3D backbone models are carried out by choosing a number of virtual microstructures with the porosity within the range of 26-64% and different combination of grain growth rate in the range of 0.001-0.999 on transversal and axial direction to the electrolyte with the same nucleation rate (0.01). The volumetric loading of particles is changed in the range of 1-25% volumetric loading. The seeding ratio that controls the distribution of particles on the surface of backbone is changed in the range of 2.5-25% of the particle. The seeding behavior, which controls the deposition probability of seed on the surface of backbone is set in two levels, free seeding or being a function of contact surface density on backbones. At last, agglomeration ratio is changed from 20-80% to simulate the aggregation of particles on the surface of the scaffold. Fig. 3 shows a small part of a 3D-realized microstructure.

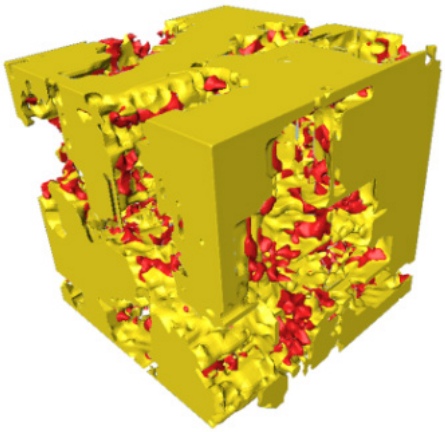

Fig. 3. A small part of realized microstructures (Backbone Porosity: 47% and volumetric loading: 5%)

Following these input specifications and their combinations, among the feasible combination of these parameters, 194 different microstructures are realized and then characterized in regard to their properties as reported in Table 1. All of these geometric parameters such as TPB and contact surface densities are evaluated directly from the mathematical model, but the tortuosity is evaluated from the 3D realized models. Among these output parameters, the exact values of TPB

Table 1. The range of output geometric variables in realized models (*L*=assumed length of voxel edge in nm)

	Unit	Min	Max	Variation
TPB density	L μm^{-2}	0.018	0.207	0.189
contact surface density of particles	L μm^{-1}	0.026	0.421	0.396
contact surface density of backbone	L μm^{-1}	0.037	0.371	0.335
contact surface density of backbone and particles	L μm^{-1}	0.009	0.256	0.247
contact surface density between particles	L μm^{-1}	0.022	0.898	0.877
pore phase tortuosity	-	1.242	7.864	6.623
average pore size	L nm	0.049	0.232	0.183
average particle size	L nm	0.006	0.020	0.013

density, contact surface density of particles and instead of tortuosity, gas diffusion factor along with input parameters are selected to train a neural network as shown in Fig. 4. It can be used to predict the properties of the each virtual microstructure for a given set of input parameters. In the current study, the extrapolation in input and output parameters is limited carefully to account for the complex behavior of fuel cells. Because of the regressive nature of the problem, a BPNN based on five inputs (backbone porosity, particle loading, seeding factor, seeding type and surface coverage behavior) and three normalized outputs (TPB Density, particle contact surface density and gas diffusion factor) is used from the Neural Network Toolbox provided in MATLAB™.
This model consists of an input layer, a hidden layer with 20

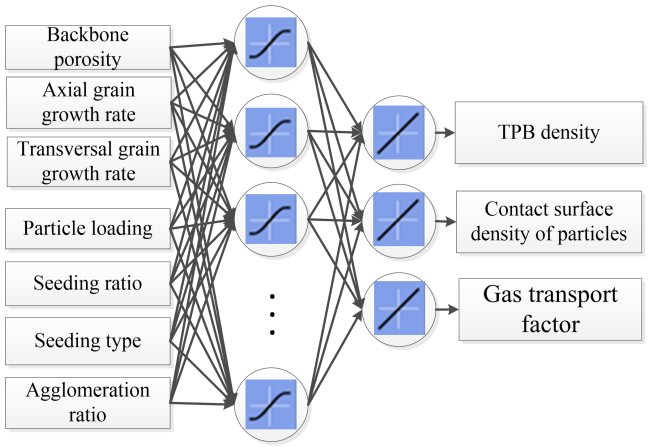

Fig. 4. The input and output parameters in the neural network structure to predict geometric properties of microstructures

neurons with tansig transfer function and an output layer with three neurons with a linear transfer function. Seventy percent of data was dedicated for neural network training using the Levenberg Marquardt algorithm and the reminded data was used to test and validate the model. The Mean Square Error (MSE) and the regression for the validation data are obtained 8.2E-5 and 0.98 in test data, respectively.

- **Optimization Scheme**

When a neural network model is trained properly, it can be used as a practical tool to predict the output parameters in terms of input variables. In other words, it would be possible to correlate the microstructure hull to property closure by sweeping feasible input variables in an acceptable range. A well-trained neural network can simulate the overall relationship between the microstructure and its properties within a limited range of input parameters. But due to complex behavior of fuel cell, this range should not be exceeded much, the previously reported input parameters to avoid improper extrapolation of data. In this way, as shown in Fig. 5, porosity, transversal and axial growth rate are divided into five levels in the ranges in backbones. Also, particle loading, seeding ratio, and agglomeration ratio are divided again into five levels and seeding type is considered in a free or confined method in virtual infiltration process.

A combination of these parameters are used to create a large number of hypothetical microstructures (~31250) to obtain a property hull using the pre-trained neural network and proposed a range of parameters in microstructure hull as listed in Table 2. This process enables researchers to predict the variation of output parameters in some specific domains that there is not any data to analyze and provide a search engine to use further optimization techniques.

Based on these input parameters, the properties of each microstructure are predicted by the neural network. Among these models, 10780 microstructures were in the range of acceptable properties with allowable positive values. The maximum and minimum property values and their range of variation are shown in Table 2. Based on the obtained properties, it is clear that the gas diffusion factor and particle contact surface density are almost 1.8 and 1.2 times more sensitive to the geometry than the TPB density regarding our assumptions. A sample property closure obtained from the predefined input parameters is shown in Fig. 6. Each axis represents one of the properties and its feasible range within the selected design space.

Based on the preferred electrochemical and physical properties of the microstructure, which resulted in the highest electrochemical sites or highest reactant gas transport, only a limited number of these microstructures can be chosen. The region of interest in the hull can be distinguished from the property closure by setting a target function. This target function is a linear (or nonlinear) combination of the microstructure properties that can be extracted from the role of materials and the rate-limiting reactions in the real microstructure in the operational condition.

From a different viewpoint, the objective function can be illustrated by a free-form surface in 3D space of the microstructure hull that separates the desirable microstructures from the rejected ones. For example, if the objective function considered being polynomial, the critical boundary is in the form of a flat plane that intercepts each 3D axis based on the coefficient of each variable in the objective function. The intersection between that plane and the microstructure hull is a border for decision making that divides the accepted or

Table 2. The range of Input and output parameters in the microstructure and property hull

		Min	Max	Variation
Input parameters	Backbone porosity	0.2	0.72	0.52
	Axial grain growth rate	0.001	0.921	0.998
	Transversal grain growth rate	0.001	0.921	0.998
	Loading of particles	0.01	0.222	0.212
	Seeding ratio	0.01	0.222	0.212
	Seeding type	0	1	-
	Surface agglomeration ratio	0.2	0.8	0.6
Output parameters	TPB density ($L\ \mu m^{-2}$)	0	0.4662	0.4662
	Contact surface density of particles ($L\ \mu m^{-1}$)	0	0.5696	0.5696
	Gas diffusion factor	0	0.8690	0.8690

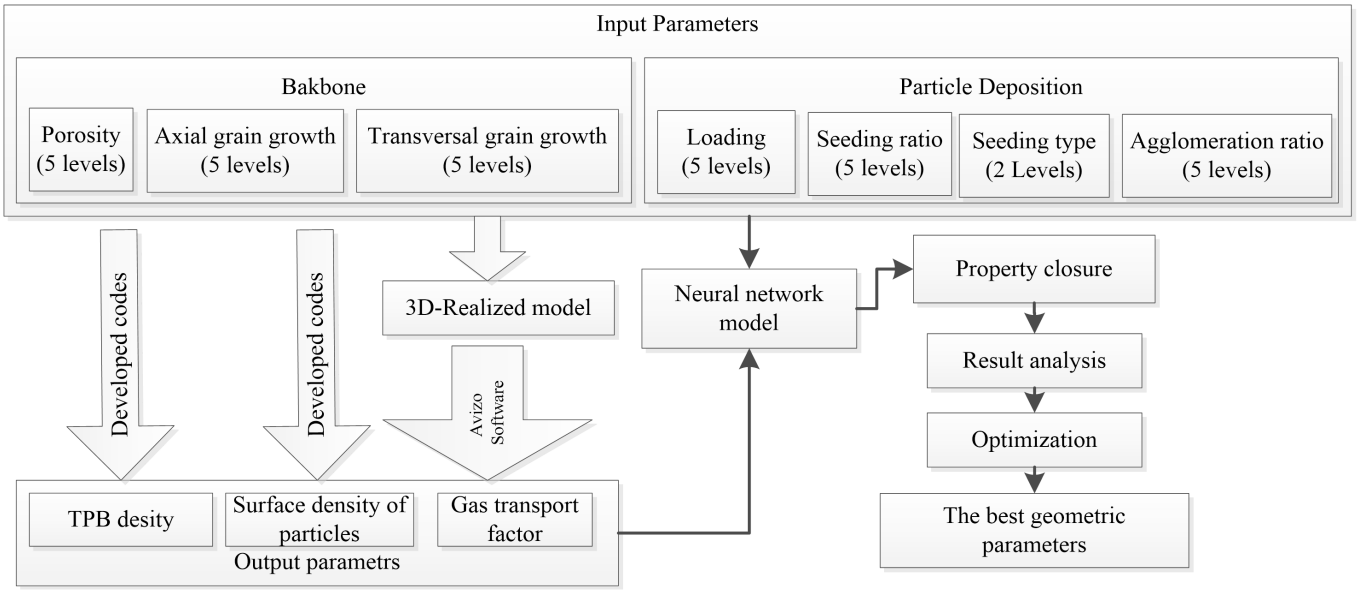

Fig. 5. Schematic diagram showing the process of geometric property prediction and optimization

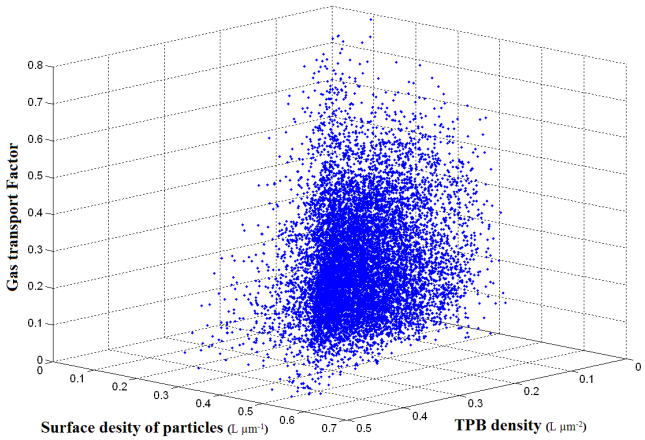

Fig. 6. Feasible Microstructures in property hull (each axis represents one of the desirable properties)

rejected microstructures. The enclosed space between the microstructure hull boundaries and objective function plane contains the appropriate microstructures. If there is not any overlap between these restricted spaces, it means that the microstructure with preferred properties does not exist due to the geometric limitation. If there is an overlapping area, an optimization method such as genetic algorithm can be used to explore the corresponding inputs parameters of these optimum microstructures. In GA, an initial population (50) of potential solutions will be randomly generated then the fitness function values will be determined and those solutions will be proportionally ranked. The new parent population will be selected among the highly ranked solutions. Some genetic operators such as crossover and mutation also will be used to combine parents and random change in new generations, up to meeting stopping criteria (reaching 100 generation or function tolerance of 1e-4). In this study, these processes are performed by the neural network Toolbox combined with the genetic algorithm multi-objective optimization Toolbox in MATLAB™ software.

4- Results and Discussion

Based on our assumptions in effective geometric properties, an ideal microstructure should have the highest active electrochemical sites (TPB & contact surface density of catalyst particles) and the maximum gas transport factor. Also, depending on the working condition of the electrode, the priority of these parameters might be varied and a combination of these parameters can be more useful to identify the best microstructures. Thus, a property closure should be detected based on different microstructures within the microstructure hull. To clarify this concept, in Fig. 7 microstructure properties are mutually compared when the third parameter is specified with color. As shown in Fig. 7a, and Fig. 7b, microstructures with the highest amount of reaction sites (TPBL or particle surface density) have a lower

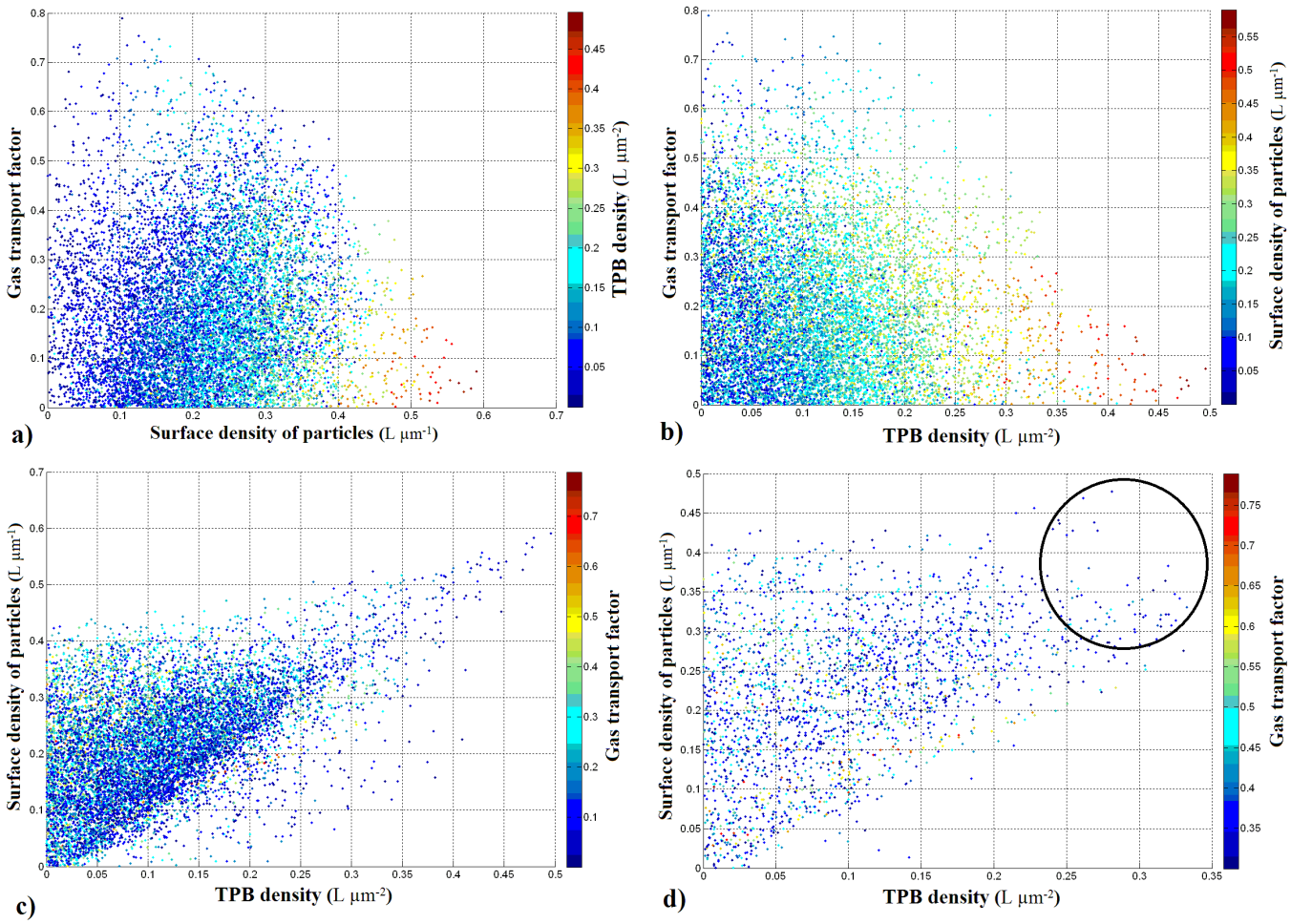

Fig. 7. Microstructure property closure comparing gas transport factor with surface density of particles (a) and TPB density (b). The surface density of microstructures with the full range (c) and feasible microstructures in high range of gas transport factor (d)

gas transport capability and may restrict the performance in some cases. A comparison between TPB density and particle surface density for hypothetical microstructures is shown in Fig. 7c. Several microstructures with the high amount of TPB density and particle surface density exist and there is not any inconsistency between these properties in the microstructure but as shown by blue points, these microstructures have a very low amount of diffusion factor. Based on these figures, a microstructure with a very high amount of both reaction sites and gas diffusion factor is not available. But a high amount of TPB density and contact surface density of catalyst particles, regardless of gas diffusion, are feasible as shown in Fig. 7c. To find a way to choose the best microstructure, a desirable level of gas transport factor can be considered. For example, if the acceptable amount of gas transport factor is set more than 0.3 (like a microstructure with the porosity of 50% and pore phase tortuosity less than 1.6), feasible TPB and particle surface density range of microstructures can be observed in Fig. 7d. The microstructures are located in the circle have the most obtainable reaction sites and acceptable level of gas diffusion.

In addition to discover the upper and lower bounds of feasible properties for a specific range of microstructures, it is possible to establish a relationship between the microstructure geometric properties and constructive variables of realized models (backbone porosity, directional growth rates, particle loading, seeding and agglomeration ratio of particles). For instance, Fig. 9 illustrates the variation of TPB density against the backbone porosity and particle volumetric loading; meanwhile, the other parameters are set fixed. It can be observed that TPB density has a maximum point by changing the particle loading. As shown in Fig. 8, there is a

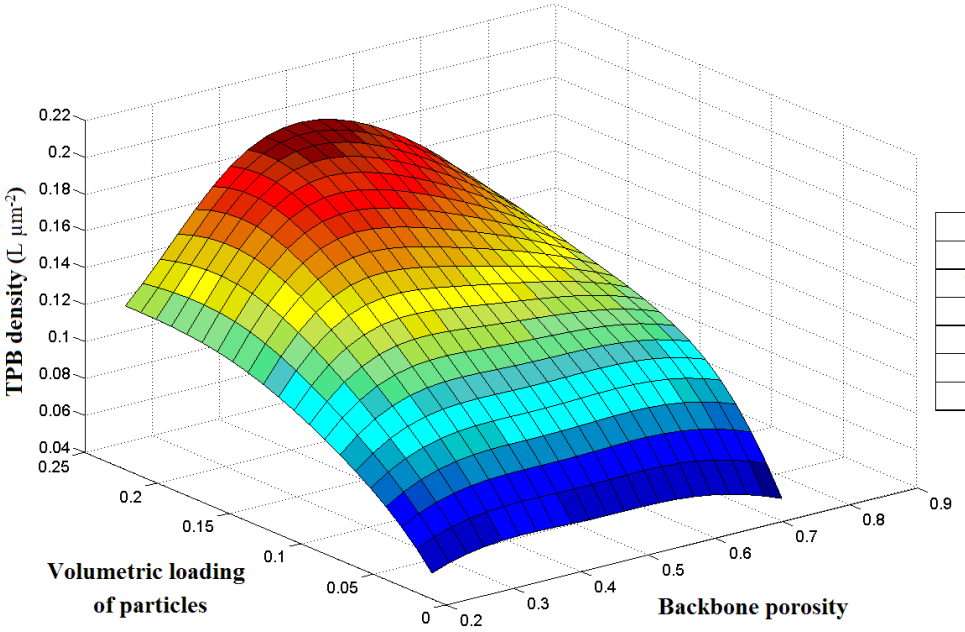

Backbone porosity	0.2 – 0.72
Axial growth	0.001
Transversal growth	0.001
Particle loading	0.01 – 0. 222
Nucleation ratio	0. 1
Nucleation type	0
Agglomeration ratio	0.7

Fig. 8. TPB density in different virtually infiltrated microstructures with various loadings and backbone porosity

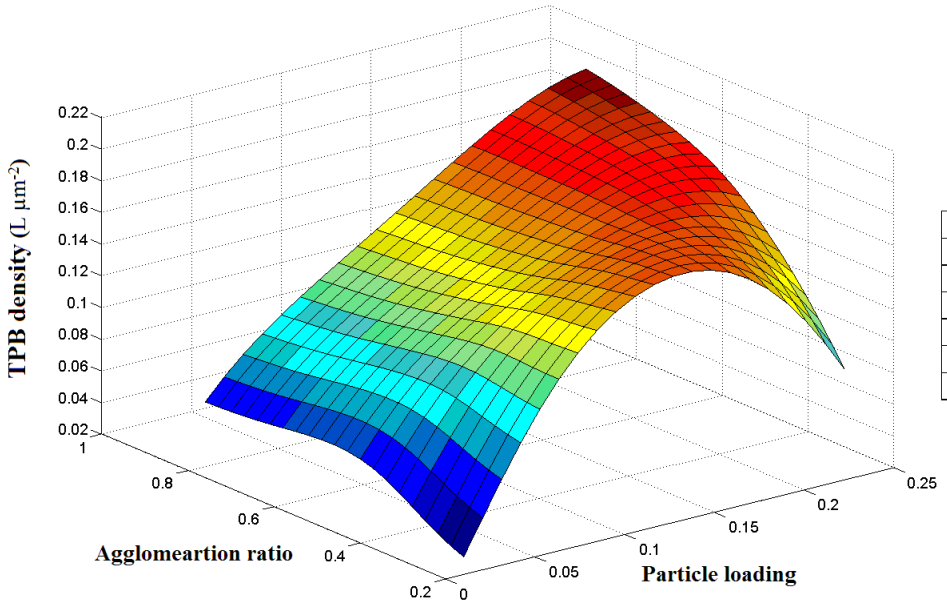

Backbone porosity	0.45
Axial growth	0.001
Transversal growth	0.001
Particle loading	0.01 – 0. 222
Nucleation ratio	0. 1
Nucleation type	0
Agglomeration ratio	0.2 – 0.8

Fig. 9. TPB density variation related to particle loading and agglomeration ratio of particles

maximum point for TPB density when the particle loading and backbone porosity are changed in proposed ranges. Also, the backbone porosity determines the variation behavior of TPB density by adding particles. In other words, very high or low level of backbone porosity constrains the maximum achievable TPB density even in the high amounts of particle loading.

The average shape of aggregated particles may play an important role in final geometric parameters of realized models. For example, as demonstrated in Fig. 9, TPB density was investigated in different microstructures by varying amount of loading and agglomeration ratio. TPB density varied in completely different trends when the particles are agglomerated over the seeds or dispersed on the surface of backbone around the primary seeds. In other words, when added particles aggregate over the seeds (in agglomerated positions), the maximum TPB density can be achieved in maximum loading, but when they are aggregated around the seeds in contact with the scaffold (in dispersed positions), there should be an optimum point for particle loading. As a result, the overall shape of infiltrated particles is an important factor in determining electrochemical site density in addition to particle loading.

The next goal of the current study is finding the optimal microstructure properties and their corresponding input constructive parameters. A simple approach is adopted here by defining a normal polynomial objective function based on the given performance indicators such as:

$$\text{Objective function} = W_1 \times (\text{TPB density}) + W_2 \times (\text{Surface density of particles}) + W_3 \times (\text{Gas transport factor}) \quad (4)$$

In this equation, the selected geometric properties have a weighting factor (W1-3) based on their roles in the performance of the electrode. Adjusting the role of each characterized property is a complicated task especially in electrochemical devices such as fuel cells whereas they depend on some external issues.

As discussed before the intrinsic property of constructive material, working condition (temperature, pressure & current density) and fuel and oxidant gas composition are the effective items in determining the impact factor of geometric properties [8,9]. For example in conventional electrodes. which consist of separate electrons and ion conductor phases, the rate of electrochemical reactions and power generation are directly related to TPB density. In infiltrated microstructures, as described before, it depends on the infiltration strategy. For example, if the backbone was made of ion conductor martial, the particles should be made of electrons conductor phase to create reaction sites at their interfaces with backbone and gas routes [1]. In this case, the TPB density can play the major role via increasing W1 in that polynomial function. On the other hand, if the backbone was made of mixed ionic electric conductor material, in addition to TBP, the contact surface density of electrode and infiltrated particles could have different effects on the rate of electrochemical reactions based on the catalytic activity of that material [10]. In this case, W2 can be considered as a critical parameter in the overall efficiency of the electrode. In addition to the density of reaction site, varying temperature and current density can change the rate limiting item [11]. To consider this state, W3 would determine the impact of reactant gas diffusion capability in electrode performance.

Generally, determining these weighting factors requires a comprehensive knowledge and is beyond the scope of the current study because of the intense discussion in that context. To simplify the optimization problem, five different scenarios over the normalized values of properties is designed. As shown in Table 3, the weighting factors are changed in those scenarios to determine the most effective parameters based on different assumptions in material roles or working conditions.

Table 3. Different optimization scenarios

scenario	Effective factor(s)	W_1	W_2	W_3
1	TPB density	1	0	0
2	Surface density of particles	0	1	0
3	Gas diffusion factor	0	0	1
4	TPB density and surface density of particles	1	1	0
5	TPB density, surface density of particles and gas diffusion factor	1	1	1

The objective function of these scenarios in combination with the proposed neural network model can directly search the microstructure hull to find the best obtainable properties for infiltrated electrodes. Table 4 reports the optimum constructive parameters of realized microstructures as well as their corresponding geometric properties based on different scenarios using direct search method in the property hull.

Table 4. The optimum microstructure based on direct search method in the microstructure and property hull

scenario		1	2	3	4	5
Micro-structural parameters	backbone porosity	0.46	0.46	0.72	0.46	0.46
	Axial grain growth rate	0.001	0.001	0.231	0.001	0.001
	Transversal grain growth rate	0.001	0.001	0.001	0.001	0.001
	Loading	0.222	0.222	0.169	0.222	0.222
	Seeding	0.169	0.169	0.222	0.169	0.116
	Seeding behavior	1	1	0	1	1
	Agglomeration ratio	0.65	0.65	0.65	0.65	0.8
Geometric property	TPB Density	0.466	0.466	0.043	0.466	0.403
	surface density of Particle	0.569	0.569	0.228	0.569	0.515
	Gas transport factor	0.060	0.060	0.869	0.060	0.316

The results indicate that if the maximum active reaction site is considered as the target function (scenarios 1, 2 and 4), the best parameters in microstructures can be 46% backbone porosity, minimum amount of directional growth rates, 22% volumetric particle loading, 17% volumetric controlled loading of seeds and the agglomeration ratio of 65%. In the third scenario, which is designed to maximize only gas transport factor, the highest level of backbone porosity and free seeding ratio are needed. The axial growth rate should set significantly more than the transversal grain growth rate and particle loading should be considered around 17%.

The fifth scenario is a combination of all output parameters in a weighted way to maximize the reaction sites and gas diffusivity simultaneously. In this way, the microstructure properties are approximately similar to first and second scenarios.

Table 5. The comparison of evaluated optimum microstructure in direct search and multi-objective genetic algorithm method base on forth scenario

Optimization scheme		GA	Direct
microstructural parameters	backbone porosity	0.59	0.46
	Axial grain growth rate	0.002	0.001
	Transversal grain growth rate	0.177	0.001
	Loading	0.222	0.222
	Seeding	0.188	0.169
	Seeding behavior	0.690	1
	Agglomeration ratio	0.218	0.65
Geometric property	TPB Density	0.449	0.466
	Particle surface Density	0.591	0.569
	Gas transport factor	0.128	0.060
	Target function	1.041	1.035

Whereas the direct search method can only search among the realized microstructures, there are more efficient approaches to find optimal microstructure using metaheuristic optimization algorithms such as genetic algorithm. To use the multi-objective genetic algorithm search method, an objective function is designed based on one of the above-mentioned scenarios. At first, the above-mentioned objective function should be converted to a fitness cost function by performing an inversion on the value (or the sign). Then to avoid impracticable extrapolation, a search domain should be defined to limit the input variable into the proposed ranges. Using multi-objective GA, in each generation of the process an optimal microstructure can be obtained. Table 5 reports one of these microstructures that meets the criteria of variation limits in the optimization algorithm under fourth scenario (maximizing the TPB and particle surface density). The total amount of TPB and surface density of particles, which is proposed as the target function, is higher in the proposed microstructure in GA method. It can be an interesting point that in that model, the gas transport factor is also improved in addition to reaction sites.

5- Conclusion

Microstructural attribution of conventional and infiltrated electrodes can significantly alter the performance of an SOFC device. The density of active electrochemical sites (TBPs and DPBs) along with the gas diffusivity of reactant gases into the microstructure is the main factors to determine the electrochemical performance of electrodes. Although in some cases the backbone ionic conductivity or electronic conductivity of particles can be rate limiting in an electrochemical process, in this study to simplify the optimization process, those are considered in an acceptable range. These parameters are linked with the backbone microstructure properties and the infiltration parameters such as loading, distribution of particles on the backbone and their agglomeration behavior. In this study, a number of 3D microstructure (more than 190) were realized by varying the porosity and directional behavior of grain in backbones, in addition to particle loading and deposition parameters to cover a wide range of possible configurations of infiltrated microstructures. An in-house algorithm was developed to calculate TPB and DPB density of particles. Furthermore, the stack of virtual cross-section images was used to evaluate the mass transport factor in the microstructures. A combination of input and output parameters was suggested to train a neural network. A microstructure hull was developed, containing a large number (~10780) of hypothetical microstructures, to obtain the property closure of all possible microstructure for a range of input geometric parameters and further optimization goals. It was observed that for the microstructures with a very high amount of TPB and surface density of infiltrated particles, a relatively low gas diffusion factor should be expected meanwhile increasing those parameters does not involve sensible contradiction. Also, it was observed that the backbone porosity determines the variation behavior of TPB density by adding particles. In addition to this, the maximum TPB density is achieved in maximum loading, when they are aggregated around the seeds in contact with the scaffold. In other words, adding particles cannot elevate the reaction sites and the overall shape of infiltrated particles determines is significantly effective in this process.

Finally, to find the best microstructure, a simple direct search scheme was used to find the optimal microstructure parameters among the members of microstructure hull with different scenarios. Then, an artificial neural network coupled with GA optimization scheme was developed to search the design space to find the best feasible geometric properties for an infiltrated electrode based on an optimization scenario. Although the results strongly depended on the definition of the objective function in different scenarios, the proposed method deemed useful to determine the limitation of available performance in experimental works and complicated interactions among microstructural parameters. This modeling approach if combined with enough experimental data and artificial intelligence can enable researchers to match the best materials and manufacturing process to get the maximum performance and durability in solid oxide fuel cell electrodes.

References

[1] N.Q. Minh, T. Takahashi, Science and technology of ceramic fuel cells, *Elsevier*, 1995.

[2] B.C. Steele, A. Heinzel, Materials for fuel-cell technologies, *Nature*, 414(6861) (2001) 345-352.

[3] N.Q. Minh, Ceramic fuel cells, *Journal of the American Ceramic Society*, 76(3) (1993) 563-588.

[4] Y. Zhang, Q. Sun, C. Xia, M. Ni, Geometric properties of nanostructured solid oxide fuel cell electrodes, *Journal of The Electrochemical Society*, 160(3) (2013) F278-F289.

[5] M. Ni, T.S. Zhao, Solid oxide fuel cells, *Royal Society of Chemistry*, 2013.

[6] M. Kishimoto, M. Lomberg, E. Ruiz-Trejo, N.P. Brandon, Enhanced triple-phase boundary density in infiltrated electrodes for solid oxide fuel cells demonstrated by high-resolution tomography, *Journal of Power Sources*, 266 (2014) 291-295.

[7] P. Shearing, D. Brett, N. Brandon, Towards intelligent engineering of SOFC electrodes: a review of advanced microstructural characterisation techniques, *International Materials Reviews*, 55(6) (2010) 347-363.

[8] H.A. Hamedani, M. Baniassadi, A. Sheidaei, F. Pourboghrat, Y. Rémond, M. Khaleel, H. Garmestani, Three-dimensional reconstruction and microstructure modeling of porosity-graded cathode using focused ion beam and homogenization techniques, *Fuel Cells*, 14(1) (2014) 91-95.

[9] V.H. Schmidt, C.-L. Tsai, Anode-pore tortuosity in solid oxide fuel cells found from gas and current flow rates, *Journal of Power Sources*, 180(1) (2008) 253-264.

[10] D.H. Jeon, J.H. Nam, C.-J. Kim, Microstructural optimization of anode-supported solid oxide fuel cells by a comprehensive microscale model, *Journal of The Electrochemical Society*, 153(2) (2006) A406-A417.

[11] S.P. Jiang, Nanoscale and nano-structured electrodes of solid oxide fuel cells by infiltration: advances and challenges, *International journal of hydrogen energy*, 37(1) (2012) 449-470.

[12] J.M. Vohs, R.J. Gorte, High-Performance SOFC Cathodes Prepared by Infiltration, *Advanced Materials*, 21(9) (2009) 943-956.

[13] Y. Zhang, M. Ni, C. Xia, Microstructural insights into dual-phase infiltrated solid oxide fuel cell electrodes, *Journal of The Electrochemical Society*, 160(8) (2013) F834-F839.

[14] A. Bertei, J.G. Pharoah, D.A. Gawel, C. Nicolella, Microstructural Modeling and Effective Properties of Infiltrated SOFC Electrodes, *ECS Transactions*, 57(1) (2013) 2527-2536.

[15] M.J. Synodis, C.L. Porter, N.M. Vo, A.J. Reszka, M.D. Gross, R.C. Snyder, A Model to Predict Percolation Threshold and Effective Conductivity of Infiltrated Electrodes for Solid Oxide Fuel Cells, *Journal of The Electrochemical Society*, 160(11) (2013) F1216-F1224.

[16] E.F. Hardjo, D.S. Monder, K. Karan, An Effective Property Model for Infiltrated Electrodes in Solid Oxide Fuel Cells, *Journal of The Electrochemical Society*, 161(1) (2014) F83-F93.

[17] A.J. Reszka, R.C. Snyder, M.D. Gross, Insights into the Design of SOFC Infiltrated Electrodes with Optimized Active TPB Density via Mechanistic Modeling, *Journal of The Electrochemical Society*, 161(12) (2014) F1176-F1183.

[18] M. Kishimoto, M. Lomberg, E. Ruiz-Trejo, N.P. Brandon, Towards the Microstructural Optimization of SOFC Electrodes Using Nano Particle Infiltration, *ECS Transactions*, 64(2) (2014) 93-102.

[19] S. Jemeı, D. Hissel, M.-C. Péra, J.-M. Kauffmann, On-board fuel cell power supply modeling on the basis of neural network methodology, *Journal of Power Sources*, 124(2) (2003) 479-486.

[20] S. Ou, L.E. Achenie, A hybrid neural network model for PEM fuel cells, *Journal of Power Sources*, 140(2) (2005) 319-330.

[21] M.T. Hagan, H.B. Demuth, M.H. Beale, O. De Jesús, *Neural network design*, PWS publishing company Boston, 1996.

[22] D. Marra, M. Sorrentino, C. Pianese, B. Iwanschitz, A neural network estimator of Solid Oxide Fuel Cell performance for on-field diagnostics and prognostics applications, *Journal of Power Sources*, 241 (2013) 320-329.

[23] S. Bozorgmehri, M. Hamedi, Modeling and Optimization of Anode-Supported Solid Oxide Fuel Cells on Cell Parameters via Artificial Neural Network and Genetic Algorithm, *Fuel Cells*, 12(1) (2012) 11-23.

[24] A. Saengrung, A. Abtahi, A. Zilouchian, Neural network model for a commercial PEM fuel cell system, *Journal of Power Sources*, 172(2) (2007) 749-759.

[25] M. Baniassadi, H. Garmestani, D. Li, S. Ahzi, M. Khaleel, X. Sun, Three-phase solid oxide fuel cell anode microstructure realization using two-point correlation functions, *Acta materialia*, 59(1) (2011) 30-43.

[26] B. Rüger, J. Joos, A. Weber, T. Carraro, E. Ivers-Tiffée, 3D electrode microstructure reconstruction and modelling, *ECS Transactions*, 25(2) (2009) 1211-1220.

[27] J. Joos, B. Rüger, T. Carraro, A. Weber, E. Ivers-Tiffée, Electrode Reconstruction by FIB/SEM and Microstructure Modeling, *ECS Transactions*, 28(11) (2010) 81-91.

[28] Q. Cai, C.S. Adjiman, N.P. Brandon, Modelling the 3D microstructure and performance of solid oxide fuel cell electrodes: computational parameters, *Electrochimica Acta*, 56(16) (2011) 5804-5814.

[29] C.W. Tanner, K.Z. Fung, A.V. Virkar, The effect of porous composite electrode structure on solid oxide fuel cell performance I. Theoretical analysis, *Journal of The Electrochemical Society*, 144(1) (1997) 21-30.

[30] Z. Jiang, C. Xia, F. Chen, Nano-structured composite cathodes for intermediate-temperature solid oxide fuel cells via an infiltration/impregnation technique, *Electrochimica Acta*, 55(11) (2010) 3595-3605.

[31] S.B. Adler, J. Lane, B. Steele, Electrode kinetics of porous mixed-conducting oxygen electrodes, *Journal of the Electrochemical Society*, 143(11) (1996) 3554-3564.

[32] A. Babaei, S.P. Jiang, J. Li, Electrocatalytic promotion of palladium nanoparticles on hydrogen oxidation on Ni/GDC anodes of SOFCs via spillover, *Journal of the Electrochemical Society*, 156(9) (2009) B1022-B1029.

[33] V.M. Janardhanan, V. Heuveline, O. Deutschmann, Three-phase boundary length in solid-oxide fuel cells: A mathematical model, *Journal of Power Sources*, 178(1) (2008) 368-372.

[34] J.S. Cronin, *Three-Dimensional Structure Combined with Electrochemical Performance Analysis for Solid Oxide Fuel Cell Electrodes*, NORTHWEStERN UNIVERSITY, 2012.

[35] N. Shikazono, D. Kanno, K. Matsuzaki, H. Teshima, S. Sumino, N. Kasagi, Numerical assessment of SOFC anode polarization based on three-dimensional model microstructure reconstructed from FIB-SEM images, *Journal of The Electrochemical Society*, 157(5) (2010) B665-B672.

[36] M. Kishimoto, M. Lomberg, E. Ruiz-Trejo, N.P.

Brandon, Towards the Design-Led Optimization of Solid Oxide Fuel Cell Electrodes, in: *ECS Conference on Electrochemical Energy Conversion & Storage with SOFC-XIV* (July 26-31, 2015), Ecs, 2015.

[37] W. He, W. Lv, J. Dickerson, *Gas transport in solid oxide fuel cells*, Springer, 2014.

[38] F. Zhao, T.J. Armstrong, A.V. Virkar, Measurement of O 2 N 2 Effective Diffusivity in Porous Media at High Temperatures Using an Electrochemical Cell, *Journal of the Electrochemical Society*, 150(3) (2003) A249-A256.

[39] D.T. Fullwood, S.R. Niezgoda, B.L. Adams, S.R. Kalidindi, Microstructure sensitive design for performance optimization, *Progress in Materials Science*, 55(6) (2010) 477-562.

[40] B.L. Adams, S. Kalidindi, D.T. Fullwood, Microstructure-sensitive design for performance optimization, *Butterworth-Heinemann*, 2013.

[41] M. Kishimoto, H. Iwai, M. Saito, H. Yoshida, Quantitative evaluation of solid oxide fuel cell porous anode microstructure based on focused ion beam and scanning electron microscope technique and prediction of anode overpotentials, *Journal of Power Sources*, 196(10) (2011) 4555-4563.

[42] A. Bertei, B. Nucci, C. Nicolella, Microstructural modeling for prediction of transport properties and electrochemical performance in SOFC composite electrodes, *Chemical Engineering Science*, 101 (2013) 175-190.

[43] M. Kishimoto, M. Lomberg, E. Ruiz-Trejo, N.P. Brandon, Numerical modeling of nickel-infiltrated gadolinium-doped ceria electrodes reconstructed with focused ion beam tomography, *Electrochimica Acta*, 190 (2016) 178-185.

[44] W. He, W. Lu, J.H. Dickerson, *Gas Transport in Solid Oxide Fuel Cells*, Springer, 2014.

Please cite this article using:

M. Tafazoli, M. Shakeri, M. Baniassadi, A. Babaei, "A Geometric Modeling Approach to Find the Best Microstructure for Infiltrated SOFC Electrodes", *AUT J. Mech. Eng.*, 1(1) (2017) 55-66.

DOI: 10.22060/mej.2017.12249.5289